Shallow Si p^+-n junctions fabricated by focused ion beam Ga^+ implantation through thin Ti and $TiSi_2$ layers

H. C. Mogul and A. J. Steckl[a)]
Nanoelectronics Laboratory, Department of Electrical and Computer Engineering, University of Cincinnati, Cincinnati, Ohio 45221-0030

S. W. Novak
Evans East, Plainsboro, New Jersey 08536

(Received 8 September 1992; accepted for publication 22 April 1993)

Focused ion beam Ga^+ implantation through Ti metal (ITM) and $TiSi_2$ (ITS) layers, followed by rapid thermal annealing (RTA), has been investigated for application in self-aligned silicide technology. The Ga^+ energy was varied from 25 to 50 keV at doses of 1×10^{13} and 1×10^{15} cm^{-2} followed by RTA at 600 °C for 30 s. Depth profiles of the Ga implants were obtained by performing secondary-ion mass spectrometry. It was observed that higher-energy and higher-dose implants yielded good quality p^+-n junction characteristics. Diodes were fabricated to obtain the electrical properties of these silicided junctions. At higher implant energies ($\geqslant$40 keV) and all doses, I-V characteristics of ITS diodes showed 100 times lower leakage currents (I_r) than ITM diodes. For low-energy ($<$40 keV)/high-dose implantation the ITS diodes showed a slight improvement in I_r over the ITM diodes, whereas for low-energy/low-dose implantation the same I_r was observed.

I. INTRODUCTION

Submicrometer complementary metal-oxide-semiconductor (CMOS) technology requires shallow junctions to minimize punchthrough and short-channel effects.[1] Recently, the self-aligned silicide (salicide) process has become widely used in metal-oxide-semiconductor (MOS) technology.[2–4] Doping by ion implantation through refractory metals and silicide layers, in conjunction with rapid thermal annealing (RTA) to complete the silicidation reaction and to remove the damage, has been utilized for the formation of ultrashallow junctions and for silicided contacts in very large scale integreted (VLSI) applications.[5,6] Shallow junctions have been formed with satisfactory results using Ti,[5] Co,[6] W,[7] and Mo.[8] Titanium silicide is one of the most promising material for the salicide technology, since it has the lowest bulk resistance of the transition metal silicides and it forms uniform thin films on Si.

Most of the current research involving salicide technology has utilized B (Refs. 4,9), BF_2 (Refs. 10,11) implantation for the formation of p^+-n junctions and As (Refs. 4,12), P (Ref. 13), implantation for n^+-p junctions. The formation of shallow p^+-n junctions currently poses a more difficult challenge for the submicron regime. In this paper, we report for the first time the use of focused ion beam (FIB) Ga^+ implantation into Ti and $TiSi_2$ as an alternative means of fabrication for salicide technology. The advantage of using Ga^+ implantation is twofold: (i) no preamorphising of the substrate is required, as in the case of B implantation,[9] since Ga is a heavy p dopant which is also very effective in providing the ion beam mixing of the metal layer; (ii) since the annealing conditions for Ga^+ activation and for the formation of $TiSi_2$ are the same ($\approx$600 °C), one can take advantage of low thermal budget processing. Thus, using Ga eliminates several processing steps required when using B implantation.[9] The FIB simplifies the process further by providing localized implantation and thereby selective silicidation with a maskless/resistless process.

II. EXPERIMENT

Shallow junction diodes were fabricated using on-axis FIB Ga^+ implantation into n-Si (100) substrates with $N_b=(5–10)\times10^{15}$ cm^{-3}. The operation of the FIB system is described elsewhere.[14] A thermal oxide of 200 nm was grown and patterned to obtain isolated diodes with area of 540×540 μm^2. A Ti layer of 10 nm was e-beam evaporated. The Ga^+ energy was varied from 25 to 50 keV at doses of 1×10^{13} and 1×10^{15} cm^{-2} using an unseparated Ga beam of 400 pA. Two schemes were employed to form the diodes: (a) implantation through metal (ITM) and (b) implantation through silicide (ITS). For the ITM scheme Ga was directly implanted through the Ti layer, while for the ITS scheme a silicide was first formed by an RTA anneal at 600 °C for 30 s, and then followed by Ga implantation. A 10 nm Ti layer is known[15] to consume 16 nm of Si to form 18 nm of $TiSi_2$. The unreacted Ti was removed in a 5:1:1 solution of H_2O:NH_4OH:H_2O_2. Selection of the implant energy was obtained by using TRIM[16] to estimate the ion stopping power of the silicide. Companion samples were prepared for making secondary-ion mass spectrometry (SIMS) measurements. SIMS was performed using a Perkin Elmer 6300 instrument with a Cs primary beam at an impact angle of 60° to reduce the ion beam mixing effect. The primary beam energy was 3 keV with a current of 205 nA. The accuracy of the SIMS measurements is within $\pm$15%. Current-voltage (I-V) measurements of the p^+-n diodes were performed using an HP4140B picoammeter controlled by an HP400 computer.

[a)]Author to whom correspondence should be addressed.

 0021-8979/93/74(4)/2318/5/$6.00 © 1993 American Institute of Physics

Downloaded 08 Oct 2003 to 129.137.210.120. Redistribution subject to AIP license or copyright, see http://ojps.aip.org/japo/japcr.jsp

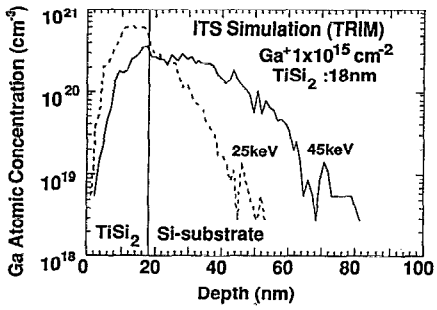

FIG. 1. The as-implanted Ga profiles obtained by TRIM simulation.

Temperature dependence of the reverse junction current was measured from 30 to 175 °C on a thermal vacuum chuck.

III. RESULTS AND DISCUSSION

A. SIMS profiles

The as-implanted Ga profiles obtained from the TRIM simulation are shown in Fig. 1 for the case of ITS samples with implant energies of 25 and 45 keV. The $TiSi_2$ film was assumed to be 18 nm thick based on the data reported in Ref. 15. The TRIM profiles show that for the case of 25 keV implant the peak depth (R_p) resides within the silicide layer while for the case of the 45 keV implant the Ga ions penetrate well within the substrate.

The actual Ga profile after annealing at 600 °C for 30 s as measured by SIMS is shown in Fig. 2 for the ITS sample implanted at 45 keV with a dose of 1×10^{15} cm^{-2}. Also shown in Fig. 2 is the Ti signal monitored during SIMS profiling. Since a standard for Ti was unavailable the intensity for the Ti profile is plotted as counts/s. Figure 2 confirms the presence of Ti atoms in the Si substrate beyond the expected thickness of the silicide layer, initially assumed to be 18 nm. This is most likely due to the ion beam mixing process, with Ga^+ ions inducing recoil implantation of Ti atoms into the substrate. This extended Ti profile was observed in all samples analyzed.

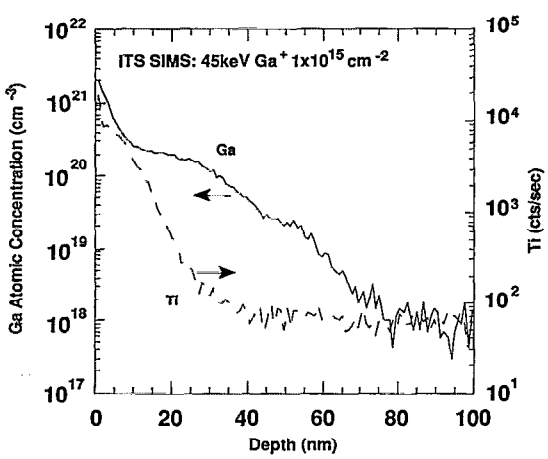

FIG. 2. SIMS profile of ITS sample with 45 keV Ga^+ implantation along with the monitored Ti signal.

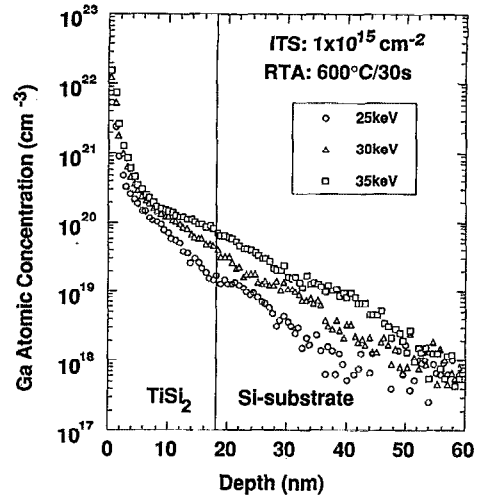

FIG. 3. SIMS profiles of the ITS sample with Ga^+ implantation at different energies to a dose of 1×10^{15} cm^{-2} followed by RTA anneal at 600 °C/30 s.

Figure 3 shows the SIMS depth profiles of the ITS samples implanted with energies between 25 and 35 keV with a dose of 1×10^{15} cm^{-2} followed by RTA at 600 °C for 30 s. For the case of the 25 keV implant it was observed that a very small percentage of the total dose penetrates through the silicide layer (D_{Si}) into the Si substrate to a concentration of 1×10^{19} cm^{-3}. It was also observed that D_{Si} increases with the implant energy from 25 to 45 keV. This increase in D_{Si} also has an effect on the current-voltage diode characteristics as will be shown in the next section. Figure 3 also shows a high surface concentration of Ga near the surface of the samples (within the first 10 nm). This high surface concentration of Ga is thought to be a real feature of the implanted sample. However, it is possible that surface contaminants may produce molecular ion interferences that mask the true Ga concentration at the surface. In addition, this surface peak is primarily within the native oxide and may represent partitioning of the Ga into the oxide during implantation. A corresponding drop in the Si signal near the surface of the sample in conjunction with the high surface concentration has also been observed with Ga implanted samples.[17] The signal reaches an equilibrium value within 2–3 nm. This drop of Si signal is due to the combination of removal of native oxide on the sample surface and the buildup of the primary beam implant within the sample. More importantly, no Ga segregration at the $TiSi_2$/Si interface was observed. This is unlike the case reported[18] for a 40 keV broad-beam Ga^+ implantation into $TiSi_2$, where after a high-temperature (1000–1100 °C) RTA annealing Ga segregation was observed at the $TiSi_2$/Si interface.

The Ga profiles for the ITM samples implanted at 35 and 45 keV with a dose of 1×10^{15} cm^{-2} are shown in Fig. 4. The same annealing condition of 30 s at 600 °C was used for each sample.

Downloaded 08 Oct 2003 to 129.137.210.120. Redistribution subject to AIP license or copyright, see http://ojps.aip.org/japo/japcr.jsp

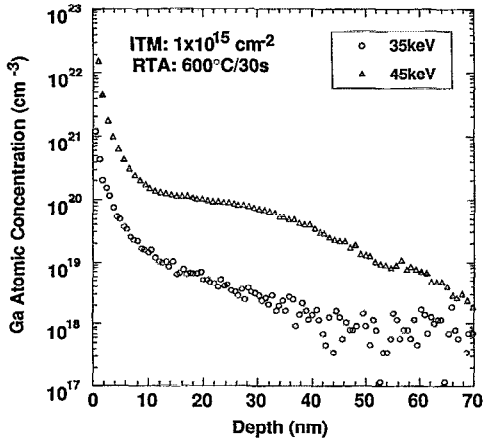

FIG. 4. SIMS profiles of the ITM sample with Ga^+ implantation at different energies to a dose of 1×10^{15} cm^{-2} followed by RTA anneal at 600 °C/30 s.

Table I summarizes the properties of the ITS diodes at various Ga^+ implantation energies: the dose which penetrates through the silicide layer in the Si substrate (D_{Si}), the Ga concentration at the $TiSi_2$/Si interface, the junction depth defined at a concentration of 1×10^{17} cm^{-3}. A thickness of 18 nm representing the silicide layer is subtracted from the junction depth values.

B. Current-voltage characteristics

Figures 5 and 6 display the current-voltage (I-V) characteristics for ITM and ITS diodes fabricated at energies ranging from 25 to 50 kV with doses of 10^{15} and 10^{13} cm^{-2}. The I-V characteristics for diodes fabricated using the ITS scheme showed 100 times lower leakage currents (I_r) at higher implant energies ($\geqslant$40 keV) and both doses when compared to ITM diodes. For the case of low-energy ($<$40 keV) and/or high-dose implants, the ITS diodes showed a decreasing improvement in I_r over the ITM diodes.

The dose dependence of I_r is related to the more complete amorphization obtained at higher doses. This, in turn, results in low defect density and low leakage current upon regrowth during anneal.

The dependence of I_r on implant energy is also partially related to amorphization and regrowth. Higher-energy implants result in higher effective doses (D_{Si}) penetrating into the Si substrate (see Table I). This not only results in fewer defects after anneal, but also in a more pronounced carrier spilling effect. This effect causes the

TABLE I. Ga concentration at $TiSi_2$/Si interface, Ga dose penetrating into the Si substrate (D_{Si}), and junction depth in ITS samples as a function of Ga implantation conditions.

ITS Ga implantation conditions E (keV)/10^{15} cm^{-2}	Ga concentration at the $TiSi_2$/Si interface (1×10^{19} cm^{-3})	D_{Si} (1×10^{13} cm^{-2})	Junction depth (nm)
25/1	1.42	3.13	33
30/1	3.66	3.36	47
35/1	7.08	6.65	55
45/1	20.5	31.7	80

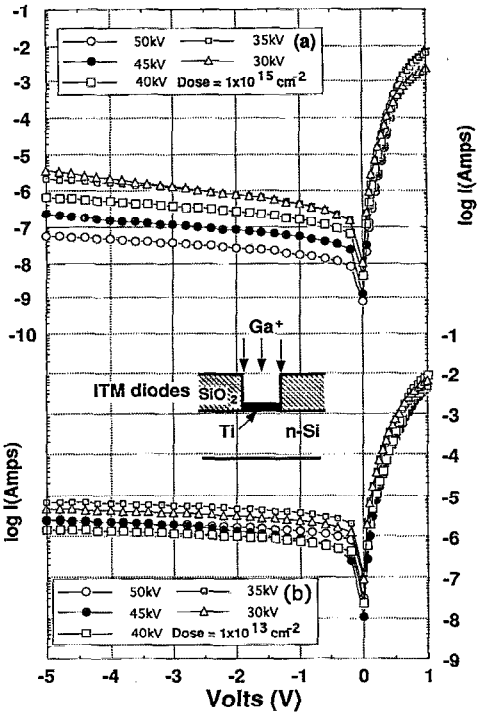

FIG. 5. I-V characteristics of FIB Ga^+ ITM diodes implanted at different energies and a dose of (a) 1×10^{15} cm^{-2} and (b) 1×10^{13} cm^{-2}.

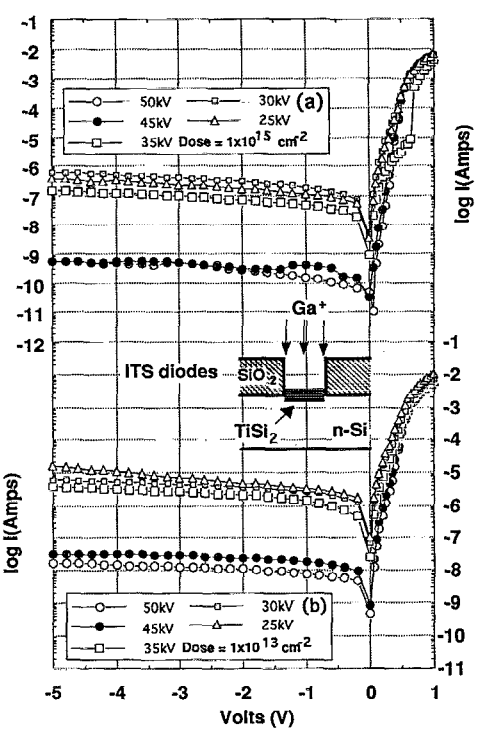

FIG. 6. I-V characteristics of FIB Ga^+ ITS diodes implanted at different energies and a dose of (a) 1×10^{15} cm^{-2} and (b) 1×10^{13} cm^{-2}.

Downloaded 08 Oct 2003 to 129.137.210.120. Redistribution subject to AIP license or copyright, see http://ojps.aip.org/japo/japcr.jsp

TABLE II. Summary of electrical properties of FIB Ga^+ ITS and ITM diodes.

	E (keV)	Dose (10^{15} cm^{-2})	I_r (−10 V) nA	I_r (−5 V) nA	I_r (−1 V) nA	n
ITS-Ga^+	50	1	1.99	0.56	0.15	1.09
ITS-Ga^+	45	1	1.3	0.55	0.41	1.3
ITM-Ga^+	50	1	128	55.4	17.5	1.7
ITM-Ga^+	40	1	1790	661.9	162	1.76
ITS-Ga^+	50	0.01	23.8	16.9	7.9	1.72
ITM-Ga^+	50	0.01	3800	2359	1300	1.98
ITS-B^+ [a]	18	1	2.13	0.5	0.15	···

[a]See Ref. 9.

defects to be located on the p^+ side of the junction and thus out of the p-n junction space-charge region, leading to smaller I_r. Comparing the leakage current in the ITM and ITS diodes, the heavily Ga^+-doped Si surface region in ITM diodes is partially consumed during annealing, thus decreasing the doping level and the x_j. This also results in some defects being located on the n side of the junction, giving rise to higher I_r. Finally, another possibility is the formation of metal-dopant compounds which can immobilize the dopant ions, thereby limiting the available dose for diffusion of the dopant into the Si substrate. This effect has been observed to lead to the degradation of the junction properties for the case of B implantation into Ti on Si[19] and for the case of Ga implantation[17] in conjunction with furnace annealing. Another factor that contributes to the leakage current for both schemes could be the presence of Ti in the space-charge region of the diodes. This argument is partially supported by the SIMS profile in Fig. 2, where one observes the progression of Ti atoms beyond the silicide layer and into the substrate.

Table II summarizes the values of I_r and ideality factor (n) for diodes fabricated by FIB Ga^+ implantation. Comparison of ITS Ga diodes fabricated by 40–50 keV/1×10^{15} cm^{-2} implantation to a Si diode fabricated[9] using B implantation through $TiSi_2$ preceded by a complex Ge preamorphization procedure indicates very similar electrical characteristics. The advantage of the present technique is that it requires significantly fewer processing steps and it results in a shallower junction depth (as compared to 230 nm from Ref. 9). Figure 7 shows the effect of temperature on I-V profiles at $T=25$, 75, 125, and 175 °C for the 45 keV ITS diodes. As shown in Fig. 8, the crossover between generation-dominated and diffusion-dominated current components occurs at ~122 °C, which compares favorably with diodes fabricated by 30 keV B implantation reported[20] to have a crossover temperature of 110 °C. The ideality factor (n) was found to be relatively insensitive to temperature between 50–125 °C ($n\approx1.7$) before increasing to 2.1 at 150 °C.

III. SUMMARY AND CONCLUSION

An investigation of the formation and characterization of p^+-n junctions using Ga as an alternative to either B or BF_2 implantation in conjunction with salicide technology was performed. Diodes were fabricated by FIB Ga^+ implantation via ITM and ITS techniques. The FIB-based implantation simplifies the process by locally implanting the required species. It was observed from SIMS depth profiling that Ga implantation results in the formation of shallow junction depths. The junction depths ranged from 30 to 90 nm depending upon the Ga^+ energy.

In general, the FIB ITS diodes yielded better electrical characteristics than the FIB ITM diodes. The FIB Ga^+-implanted ITS diodes have I_r values comparable to those of diodes[9] fabricated with broad beam B^+ implanta-

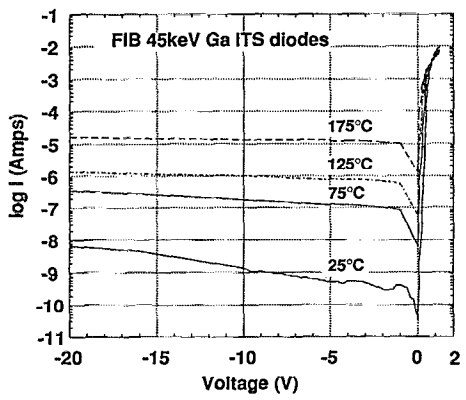

FIG. 7. Temperature dependence of 45 keV/1×10^{15} cm^{-2} FIB Ga^+ ITS diode I-V characteristics.

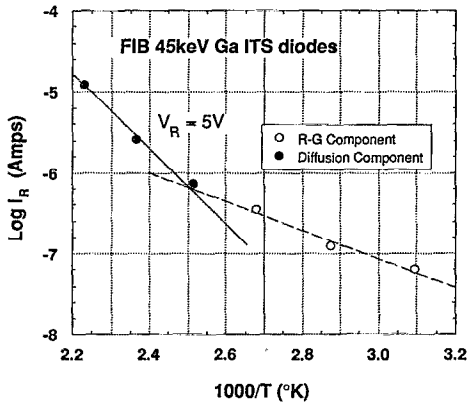

FIG. 8. Temperature dependence of leakage current at $V_R=5$ V for 45 keV/1×10^{15} cm^{-2} FIB Ga^+ ITS diode.

Downloaded 08 Oct 2003 to 129.137.210.120. Redistribution subject to AIP license or copyright, see http://ojps.aip.org/japo/japcr.jsp

tion into $TiSi_2$, but with a shallower x_j and a simpler process. A dependence of the leakage current on dose at a given energy was observed, namely that the leakage current decreased with increasing dose. This is partly due to complete amorphization of the substrate occuring at a high dose leading to a higher activation and lower damage upon anneal.

The best electrical characteristics were obtained with ITS diodes implanted at higher energy and high dose, followed by ITS diodes implanted at high energy and low dose and by ITM diodes implanted at high energy and high dose.

[1] R. B. Fair, Proc. IEEE **78**, 1687 (1990).
[2] C. Lau, Y. See, D. Scott, J. Bridges, S. Perna, and R. Daines, IEDM Tech. Dig. 714 (1982).
[3] M. Alperin, T. Halloway, R. Hakin, C. Gosmeyer, R. Karnaugh, and W. Paramanti, IEEE J. Solid State Circuits **SC-20**, 61 (1985).
[4] L. Rubin, D. Hoffman, D. Ma, and N. Herbots, IEEE Trans. Electron Devices **ED-37**, 183 (1990).
[5] D. Wong, Y. Ku, S. Lee, E. Louis, N. Alvi, and P. Chu, J. Appl. Phys. **61**, 5084 (1987).
[6] L. Van den Hove, R. Wolters, K. Maex, R. de Keersmaecker, and G. Declerk, IEEE Trans. Electron Devices **ED-34**, 554 (1987).
[7] B. Tsaur, C. Chen, C. Andersoon, and D. Kwong, J. Appl. Phys. **57**, 1980 (1985).
[8] R. Angelucci, S. Solmi, A. Armigliato, E. Gagilli, D. Govoni, M. Merli, and A. Poggi, Solid-State Electron. **35**, 941 (1992).
[9] C. Dehm, E. Burte, J. Gyulai, and H. Zimmerman, J. Appl. Phys. **71**, 4365 (1992).
[10] M. Juang and H. Cheng, Solid-State Electron. **35**, 453 (1992).
[11] J. Choi, Y. Hwang, S. Paek, J. Oh, T. Sim, and J. Lee, J. Appl. Phys. **72**, 297 (1992).
[12] C. Lu, J. Sung, R. Liu, N. Tsai, R. Singh, S. Hillenius, and H. Kirsch, IEEE Trans. Electron Devices **ED-38**, 246 (1991).
[13] M. Juang and H. Cheng, Appl. Phys. Lett. **60**, 1579 (1992).
[14] A. J. Steckl, H. C. Mogul, and S. Mogren, J. Vac. Sci. Technol. B **8**, 1937 (1990).
[15] D. Chen, IEDM Tech. Dig. 41 (1985).
[16] J. Ziegler, J. Biersack, and U. Littmark, *Stopping and Range of Ions in Matter* (Pergamon, New York, 1988), Vol. I.
[17] S. W. Novak, C. W. Magee, H. C. Mogul, and A. J. Steckl, J. Vac. Sci. Technol. B **10**, 333 (1992).
[18] P. Lippens, K. Maex, L. Van den Hove, and R. De Keersmaecker, Nucl. Instrum. & Methods B **39**, 330 (1989).
[19] V. Probst, H. Schaber, A. Mitwalsky, H. Kabza, B. Hoffman, K. Maex, and L. Van den Hove, J. Appl. Phys. **70**, 708 (1991).
[20] J. Lasky, J. Appl. Phys. **54**, 6009 (1983).

Downloaded 08 Oct 2003 to 129.137.210.120. Redistribution subject to AIP license or copyright, see http://ojps.aip.org/japo/japcr.jsp